Available online at www.sciencedirect.com

ScienceDirect

Procedia Structural Integrity 52 (2024) 105–110

Structural Integrity Procedia

www.elsevier.com/locate/procedia

Fracture, Damage and Structural Health Monitoring

Mechanical Degradation and Fatigue Life of Amorphous Polymers

Thierry Barriere[a], Xavier Gabrion[a], Najimi Imane[a], Sami Holopainen[b,*]

[a] *FEMTO-ST Institute, Applied Mechanics Department, 24 Rue de l'Epitaphe, 25000 Besancon, France*
[b] *Tampere University, Department of Civil Engineering, FI-33014 Tampere, Finland*

Abstract

Due to favorable properties (cheap price, easy processing, preeminent combination of toughness and strength, clearness, recyclability etc.), amorphous polymers are widely used in windows, sporting goods, vehicles, aeronautic equipment, electronics, and health technology. However, their applications may suffer from fatigue, when material fails at significantly lower stress levels than under monotonic loading conditions; fatigue loads result in polymer degradation which can affect horrific accidents (e.g., the air disaster of China Airlines Flight 611) and tremendous financial losses. Despite this motivation, fatigue behavior of amorphous polymers has been scarcely investigated so far. In this study, micro-mechanical characteristics of amorphous structure and their influence on macroscopic deformation behavior (ratcheting) and fatigue life are investigated. It was found (SEM results) that polymer degradation is the process of failure (shear banding affecting micro-cracking and fracture) causing finally breakdown of polymer network. The degradation process was very rate sensitive, and the crack initiation phase before rapid rupture of the material encompassed the majority (even 95 %) of the total fatigue life. Certain fracture surfaces showed sharpened protrusions indicating that the separation of the fracture surfaces from each other occurred precisely on those protrusions. The vein-like, cellular, and rippled patterns of shear bands on fracture surfaces increased fracture toughness and thus, fatigue resistance and life.

Keywords: Fatigue; Polymers; Cyclic viscoplasticity; Ratcheting

1. Introduction

When applying materials in practise, attention inevitably focuses on their resistance over the service life. Many applications are subjected to fatigue loads when their fatigue resistance must be investigated. This typically requires various experimental tests to be conducted. However, such an experimentation is costly and time-consuming, and thus, it is also worth developing capable models to simulate resource-intensive tests and to develop improved materials and their manufacturing processes Holopainen and Barriere (2018); Bennett and Horike (2018); Barriere et al. (2019, 2021); Zirak and Tcharkhtchi (2023). The development of an advanced, realistic fatigue model as well as fatigue resistant materials requires a deep knowledge of the micromechanical behavior of the material. Notable con-

* Corresponding author.
E-mail address: sami.holopainen@tuni.fi

10.1016/j.prostr.2023.12.011

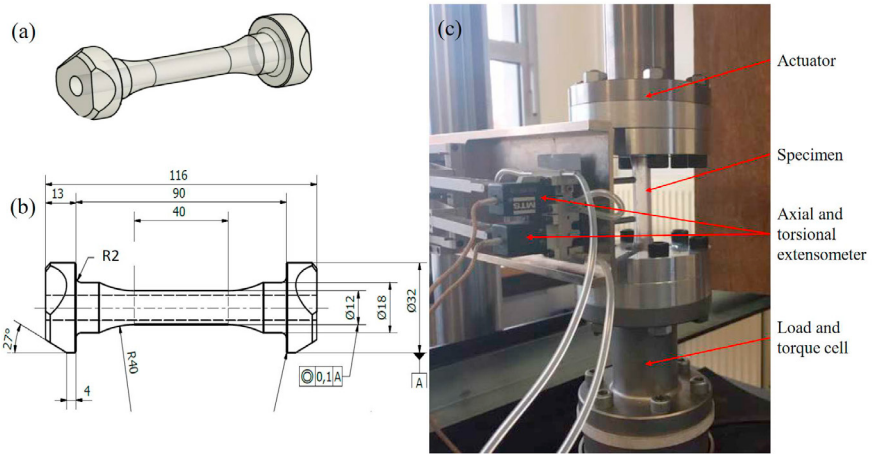

Figure 1. (a) Design and (b) dimension (mm) of the test specimen. (c) The testing setup.

tribution has been conducted to describe the progress of fatigue failure by mechanical tension/compression tests Chen et al. (2015); Lu et al. (2016); Krairi et al. (2019) and molecular dynamics simulation Bao et al. (2020). However, although amorphous polymers have a vast number of applications Lu et al. (2016); Kang and Kan (2017); Lei and Wu (2019); Bennett and Horike (2018), little work has been conducted on the experimental investigation of their microstructural characteristics under fatigue loads Hertzberg et al. (1970); Janssen et al. (2008b); Lu et al. (2016); Kanters et al. (2016); Bennett and Horike (2018); James et al. (2013); Ravi Chandran (2016); Hughes et al. (2017); Kamal et al. (2022). As an example, finding for articles with terms *"amorphous polymers" fatigue micro*, ScienceDirect (`https://www.sciencedirect.com/`) resulted only about 200 results (time span 2018-22). In this study, attention is focused on this issue, that is, microstructural mechanical degradation and its influence on the fatigue life of amorphous polymers are investigated.

2. Methods

A thermoplastic mold with specific die cavities (based on ASME standard) was manufactured for injecting the test specimens Barriere et al. (2018). The injection was realized with a dry polycarbonate (PC) Lexan® 223R granulate, with a density of 1.2 g/cm^3. Using differential scanning calorimetry (DSC), the complete amorphous nature was verified, and the injected specimens had the same physical properties as the granulate. The geometry of the specimens is demonstrated in Fig. 1 and it is in compliance with the standard ASTM E2207 (2002). This specimen geometry, also available for torsion, is very stable under tension, that is, more numb to necking phenomenon than a standard tensile specimen ASTM D2990 (2001); ASTM D638 (2003). Since the results of the fatigue tests are susceptible to sample errors, particular attention was paid to the quality of the specimens: the flaws were analyzed by Werth video-inspection and X-ray tomography, and the high quality of the shape was verified by using optic 3D metrology (Alicona analyzer). The detected surface faults were under 0.03 mm, when their effect on the test results can be regarded as infinitesimal because the inaccuracies they affected in the outer radius (6 mm) of the gauge section and the cross-section are only 0.5 % and 1.1 %, respectively.

Experimental observations were made of cyclic uniaxial tensile tests. The tests and observations took place at room temperature (RT). The degradation process was very rate sensitive, and the cyclic quasi-static tests were performed by load-control at the frequency of 5 Hz either until rupture or until prescribed cycles 500, 1000, 1500, 3500, and 5000 in order to investigate the propagation of failure mechanisms during fatigue loads. An Instron® test machine having a load capacity of 10 kN and a displacement capacity of ±30 mm was used, and the stress was allowed to vary between 4...40 MPa, when the maximum stress was 75 % of the ultimate tensile yield strength, ~60 MPa. It should

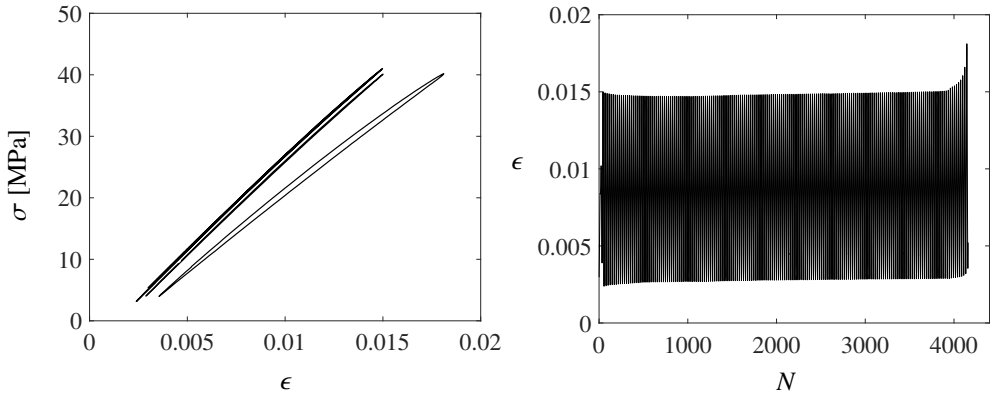

Figure 2. Representative observed stress vs. strain responses for 1...3, 3500, and 4160 (right prior to rupture) cycles (left). The corresponding development of strain during cycles (right).

be noticed that PC shows plastic deformation and yielding right once a loading is applied Dreistadt et al. (2009); Holopainen (2013); Holopainen et al. (2017). The force F and the corresponding axial elongation u were recorded by the testing machine according to the standard D2990-01. Moreover, the axial elongation was measured by an extensometer (Instron® with the capacity of 5 mm), which, to avoid slipping, was securely glued onto the surface of the gauge section. To ensure the reliability of the results, each test was repeated at least once. The nominal stress $\sigma = F/A$ was used because it is easy to measure and calculate: recorded force F divided by the original cross-sectional area A of the tubular gauge section. The error in relation to the true Cauchy stress is small because the cyclic strains remain relatively small (less than 3 %) and the difference between the measured cross-sectional areas before and after the tests was small. The strain was calculated as $\epsilon = u/L$, where $L = 4$ mm is the gauge length of the extensometer applied.

Investigation and prediction of the fatigue life are possible through the analysis of the microstructural fatigue failure mechanisms consisting of the initiation and propagation of cracks Janssen et al. (2008a); Pastukhov et al. (2020); Chudnovsky et al. (2012); Zirak and Tcharkhtchi (2023). Scanning electron microscope (SEM) imaging was performed during and after the tests to observe the micromechanical mechanisms and progress of fatigue failure. The SEM imaging was performed from the surface of the gauge section of the specimens, except after the ruptured tests, where the imaging was performed also from the ruptured cross-sectional surfaces.

3. Results

The load-controlled fatigue tests described above were designed to observe the initial strain followed by strain softening (the first, primary stage), stabilized secondary stage, and ratcheting (the third tertiary cyclic creep stage), see Fig. 2. Moreover, the elastic modulus E, measured during the first cycle (initial stress divided by the corresponding strain), is about 2000 MPa. It was observed that the peak yield strain, present at the beginning of loading, is approximately 10 % greater than the stabilized strain after softening. Moreover, after the second stage, strains rapidly accumulate right before rupture referring to ratcheting and, due to tension, a plastic instability termed necking. The corresponding degradation process before rapid rupture of the material (the primary and secondary stages) encompassed the majority (even 95 %) of the total fatigue life. The question arises as to which microstructural changes cause the observed macroscopic deformation behavior and fatigue life.

Fig. 3(left) shows that shear bands (SBs) initiate from impurities or some flakes in the material and cause a onset of fatigue failure. After continued cyclic loads, SBs enlarge and the most ones show crazing or initial cracks, Fig. 3(middle). Crazing, i.e., changes in the fibril or chain disentanglement, explains the origin of plastic deformation Venkatesan and Basu (2015); Zirak and Tcharkhtchi (2023). Previous experiments also show fractographic details that the hypothesis that plastic deformation in localized SBs is a precursor to initial cracking James et al. (2013). These two failure mechanisms, shear banding and crazing, cause an increase of void volume (loosely packed regions in the

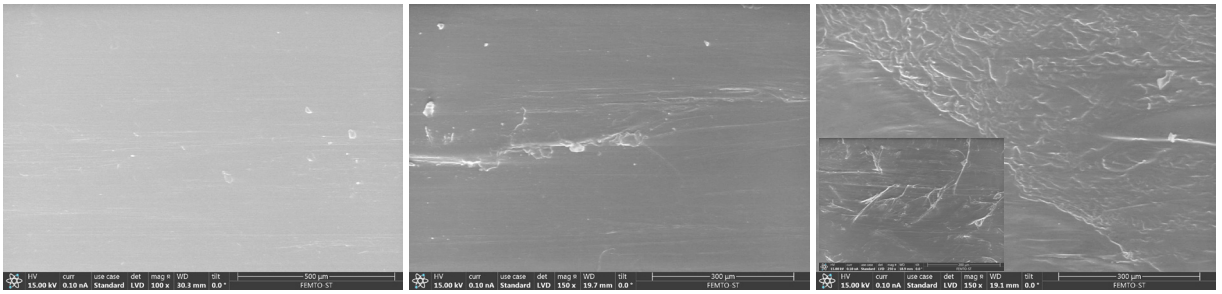

Figure 3. Microstructure at 500 cycles (left), 1500 cycles (middle), and 3500 cycles (right) (local SBs are shown in the inset; the specimen broke at 4820 cycles).

material which are also associated to free volume in nano-scale Barriere et al. (2019)). Crazing is further generated in regions of high void volume Venkatesan and Basu (2015), i.e., the void volume and initiation of plastic deformation through crazing are interconnected. In conclusion, in line with the previous research Ravi Chandran (2016), the fatigue failure in amorphous polymer structure develops through the mechanism of cyclic fracturing of fibrils (crazing) leading to accumulated void volume fraction and cracking James et al. (2013). The growth of void volume (free volume) has been reported to be strongest at crack tips, that is around impurities where crazing develops Holopainen (2014); Ravi Chandran (2016). Once majority of the fatigue life (~60 %) is reached, vein-like and rippled zones of SBs start to develop, preventing enlarging of the micro-cracks James et al. (2013), see Fig. 3(right). This microstructural characteristic explains the long-term stable deformation behavior before ratcheting and rupture shown in Fig. 2.

Important microstructural graphs of ruptured specimens after the tests are shown in 4. Enlarged, curved, and rather parallel cracks govern the fracture surfaces. What is striking is that the fracture surfaces have sharpened protrusions, Fig. 4(middle). This phenomenon shows that the separation of the fracture surfaces from each other has occurred precisely on those protrusions. Fig. 4(right) further shows a large crack which formed among the last cracks before rupture. Therein vein-like, cellular, and rippled zones of SBs occur around the fracture surfaces limiting the enlargement of the fracture surfaces.

Fig. 5(left-middle) shows an alternative, discontinuous propagation of fatigue failure observed between the gauge section and the hold part of the specimen (occurred solely at higher numbers of cycles about 5000 for rupture). That is, the initiation and propagation of this form of fatigue failure depend on both the impurities in the material and the geometry of the specimen. A fracture surface shows repetitive curved streaks, and, based on the comparison of different number of cycles, the number of streaks increases during loading cycles, i.e., the streaks progress and expand in cycles. The observed pattern gradually vanishes beyond its initiation zone and is replaced by vein-like and rippled zones of SBs shown in Fig. 5(right) preventing further failure. Moreover, the distance or gaps (~5 μm) between two successive streaks is virtually constant, and the shape (thickness and height) of the two successive streaks also seemed to be rather similar. It should be noticed that the zone between two streaks is homogeneous and the streaks are governed by SBs affecting failure. The similar fatigue failure behavior has previously been reported in Zirak and Tcharkhtchi (2023); the more the streaks advances, the higher the development of fatigue failure and the local stress concentration at the streak front.

4. Conclusions

The forms vein-like, cellular, and rippled zones of SBs prevented the opening of fracture surfaces and therefore, are in pursuit to increase the fatigue resistance and life. In addition to cracks, certain fracture surfaces showed repetitive, curved streaks, and the number of streaks increased during loading cycles. A possibility to estimate the fatigue life through the number of streaks and the number of cycles between the streaks is definitely an important matter to be investigated in future. The difference of the distances between two successive streaks in the initiation zone and in the zone at the end of propagation (prior to rupture) is probably the most important factor for defining the number of cycles and fatigue life.

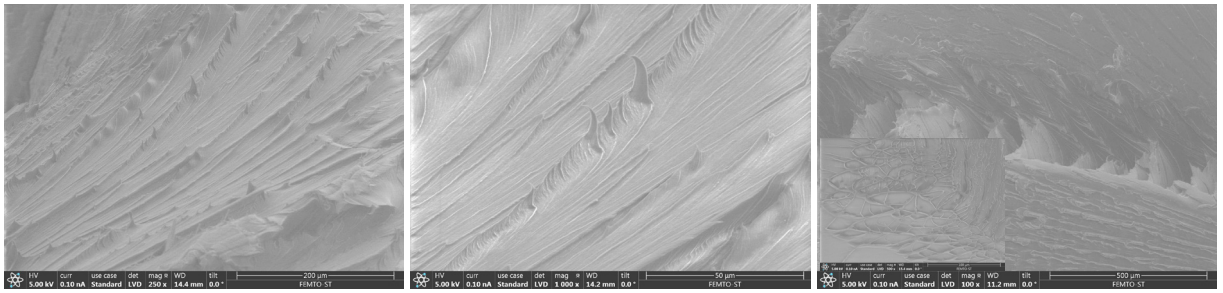

Figure 4. Microstructure of a fracture surface in a ruptured specimen at 3190 (left-middle) and at 4820 cycles (right) (local structure is shown in the inset).

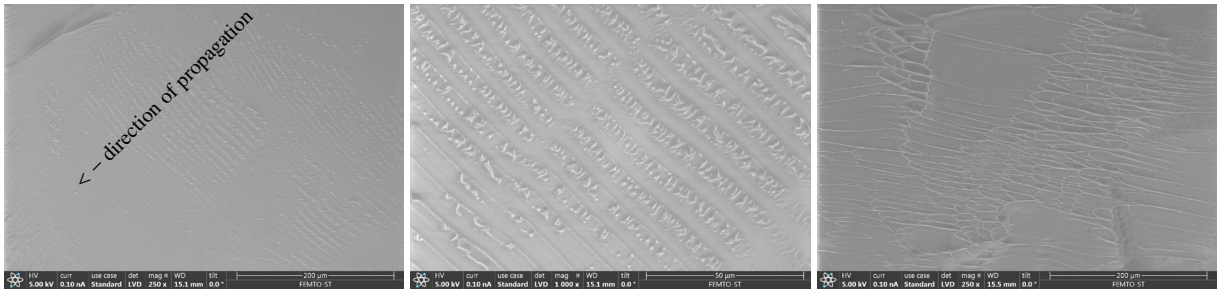

Figure 5. Second ruptured microstructure (left-middle) at 4820 cycles. The pattern gradually vanishes and is replaced by vein-like and rippled zones of SBs (right).

Acknowledgements

We thank Dr. S. Carbillet for contributing experimental facilities.

References

ASTM D2990, 2001. Standard test methods for tensile, compressive, and flexural creep and creep- rupture of plastics. ASTM International, ICS Code: Non, 1–20.

ASTM D638, 2003. Designation: D 638 - 03. Standard test method for tensile properties of plastics. ASTM International, ICS Code: 83.080.01, 1–15.

ASTM E2207, 2002. Standard practice for strain-controlled axial-torsional fatigue testing with thin- walled tubular specimens. ASTM International, ICS Code: Non, 1–8.

Bao, Q., Yang, Z., Lu, Z., 2020. Molecular dynamics simulation of amorphous polyethylene (PE) under cyclic tensile-compressive loading below the glass transition temperature. Polymer 186, 121968.

Barriere, T., Cheng, G., Holopainen, S., 2018. Modeling, simulation, and experimentation of fatigue behavior in amorphous solids. Key Eng. Mat. 774, 210–216.

Barriere, T., Gabrion, X., Holopainen, S., 2019. A compact constitutive model to describe the viscoelastic-plastic behaviour of glassy polymers: Comparison with monotonic and cyclic experiments and state-of-the-art models. Int. J. Plasticity 122, 31–48.

Barriere, T., Gabrion, X., Holopainen, S., 2021. Short- to long-term deformation behavior, failure, and service life of amorphous polymers under cyclic torsional and multiaxial loadings. Int. J. Plasticity 147, 103106.

Bennett, T.D., Horike, S., 2018. Liquid, glass and amorphous solid states of coordination polymers and metal-organic frameworks. Nat. Rev. Mater. 3, 431–440.

Chen, G., Liang, H.Q., Wang, L., Mei, Y.H., Chen, X., 2015. Multiaxial ratcheting-fatigue interaction on acrylonitrile-butadiene-styrene terpolymer. Polym. Eng. Sci. 55, 664–671.

Chudnovsky, A., Zhou, Z., Zhang, H., Sehanobish, K., 2012. Lifetime assessment of engineering thermoplastics. Int J Eng Sci Elsevier 59, 108–39.

Dreistadt, C., Bonnet, A.S., Chevrier, P., Lipinski, P., 2009. Experimental study of the polycarbonate behaviour during complex loadings and comparison with the Boyce, Parks and Argon model predictions. Materials and Design 30, 3126–3140.

Hertzberg, R.W., Nordberg, H., Manson, J.A., 1970. Fatigue crack propagation in polymeric materials. J Mater Sci Springer 5, 521–526.
Holopainen, S., 2013. Modeling of the mechanical behavior of amorphous glassy polymers under variable loadings and comparison with state-of-the-art model predictions. Mechanics of Materials 66, 35–58.
Holopainen, S., 2014. Influence of damage on inhomogeneous deformation behavior of amorphous glassy polymers. Modeling and algorithmic implementation in a finite element setting. Engng. Fract. Mech. 117, 28–50.
Holopainen, S., Barriere, T., 2018. Modeling of mechanical behavior of amorphous solids undergoing fatigue loadings, with application to polymers. Computers and Structures 199, 57–73.
Holopainen, S., Barriere, T., Cheng, G., Kouhia, R., 2017. Continuum approach for modeling fatigue in amorphous glassy polymers. applications to the investigation of damage-ratcheting interaction in polycarbonate. Int. J. Plasticity 91, 109–133.
Hughes, J.M., Lugo, M., Bouvard, J.L., McIntyre, T., Horstemeyer, M.F., 2017. Cyclic behavior and modeling of small fatigue cracks of a polycarbonate polymer. Int. J. Fatigue 99, 78–86.
James, M.N., Lu, Y., Christopher, C.J., Patterson, E.A., 2013. Crack path support for deformation mechanisms in fatigue of polycarbonate. Engng. Fract. Mech. 108, 89–97.
Janssen, R.P.M., Govaert, L.E., Meijer, H.E.H., 2008a. An analytical method to predict fatigue life of thermoplastics in uniaxial loading: Sensitivity to wave type, frequency, and stress amplitude. Macromolecules 41, 2531–40.
Janssen, R.P.M., Kanter, D.K., Govaert, L.E., Meijer, H.E.H., 2008b. Fatigue life predictions for glassy polymers: A constitutive approach. Macromolecules 41, 2520–30.
Kamal, A., Showaib, E., Elsheikh, A., 2022. Effect of single-period overload parameters on fatigue crack retardation for high-density polyethylene. Theor Appl Fract Mech Elsevier 118, 103249.
Kang, G., Kan, Q., 2017. Cyclic Plasticity of Engineering Materials: Experiments and Models. John Wiley & Sons, Chichester.
Kanters, M.J.W., Kurokawa, T., Govaert, L.E., 2016. Competition between plasticity-controlled and crack-growth controlled failure in static and cyclic fatigue of thermoplastic polymer systems. Polymer Testing 50, 101–110.
Krairi, A., Doghri, I., Schalnat, J., Robert, G., Van Paepegem, W., 2019. Thermo-mechanical coupling of a viscoelastic-viscoplastic model for thermoplastic polymers: Thermodynamical derivation and experimental assessment. Int. J. Plasticity 115, 154–177.
Lei, Z., Wu, P., 2019. A highly transparent and ultra-stretchable conductor with stable conductivity during large deformation. Nat. Commun. 10, 3429.
Lu, F., Kang, G., Zhu, Y., Xi, C., Jiang, H., 2016. Experimental observation on multiaxial ratchetting of polycarbonate polymer at room temperature. Polymer Testing 50, 135–144.
Pastukhov, L.V., Kanters, M.J.W., Engels, T.A.P., Govaert, L.E., 2020. Physical background of the endurance in poly(ether ether ketone). J Polym Sci. , 1–21.
Ravi Chandran, K.S., 2016. Mechanical fatigue of polymers: A new approach to characterize the S-N behavior on the basis of macroscopic crack growth mechanism. Polymer 91, 222–238.
Venkatesan, S., Basu, S., 2015. Investigations into crazing in glassy amorphous polymers through molecular dynamics simulations. J. Mech. Phys. Solids 77, 123–145.
Zirak, N., Tcharkhtchi, A., 2023. Fatigue life prediction for amorphous glassy polymers based on cumulative evolution of micro-defects. Int. J. Fatigue 167, 107360.